



Contents lists available at ScienceDirect

## Progress in Oceanography

journal homepage: [www.elsevier.com/locate/pocean](http://www.elsevier.com/locate/pocean)

## Intraseasonal variation in southeast Pacific blue whale acoustic presence, zooplankton backscatter, and oceanographic variables on a feeding ground in Northern Chilean Patagonia

Susannah J. Buchan<sup>a,b,c,\*</sup>, Iván Pérez-Santos<sup>a,d,f</sup>, Diego Narváez<sup>a,b</sup>, Leonardo Castro<sup>a,b</sup>, Kathleen M. Stafford<sup>g</sup>, Mark F. Baumgartner<sup>c</sup>, Arnoldo Valle-Levinson<sup>h</sup>, Paulina Montero<sup>a,f</sup>, Laura Gutiérrez<sup>a,e</sup>, Constanza Rojas<sup>i</sup>, Giovanni Daneri<sup>a,f</sup>, Sergio Neira<sup>a,b</sup>

<sup>a</sup> Centro de Investigación Oceanográfica COPAS Sur-Austral and COPAS Coastal, Universidad de Concepción, Casilla 160-C, 4070043, Concepción, Región del Bio, Chile

<sup>b</sup> Departamento de Oceanografía, Facultad de Ciencias Naturales y Oceanográficas, Universidad de Concepción, Casilla 160-C, 4070043, Concepción, Región del Bio, Chile

<sup>c</sup> Woods Hole Oceanographic Institution, Biology Department, 266 Woods Hole Road, Woods Hole, MA 02543, USA

<sup>d</sup> Centro i-mar, Universidad de Los Lagos, Camino a Chinquihue km 6, Puerto Montt, Región del Los Lagos, Chile

<sup>e</sup> Graduate Program in Oceanography, Departamento de Oceanografía, Facultad de Ciencias Naturales y Oceanográficas, Universidad de Concepción, Casilla 160-C, 4070043, Concepción, Región del Bio, Chile

<sup>f</sup> Centro de Investigaciones en Ecosistemas de la Patagonia (CIEP), José de Moraleda 16, Coyhaique, Región de Aysén, Chile

<sup>g</sup> Applied Physics Laboratory, University of Washington, Henderson Hall, 1013 NE 40th St., Seattle, WA 98105, USA

<sup>h</sup> University of Florida, Civil and Coastal Engineering Department, 365 Weil Hall, PO Box 116580, Gainesville, FL 32611-6580, USA

<sup>i</sup> Undergraduate Program in Marine Biology, Pontificia Universidad Católica de Chile, Av Libertador Bernardo O'Higgins 340, Santiago, Región Metropolitana, Chile

## ARTICLE INFO

## Keywords:

Blue whales  
Euphausiids  
Passive acoustics  
Active acoustics  
Estuaries  
Backscatter  
Tidal forcing  
Wind stress

## ABSTRACT

Seasonal variation in the acoustic presence of blue whale calls has been widely reported for feeding grounds worldwide, however variation over the submonthly scale (several days to <1 month) has been examined to a much lesser extent. This study combines passive acoustic, hydroacoustic, and *in situ* oceanographic observations collected at a mooring in the Corcovado Gulf, Northern Chilean Patagonia, from January 2016–February 2017, to examine the temporal variation in blue whale acoustic occurrence and prey backscatter over seasonal and submonthly scales. Time series data for a) Southeast Pacific blue whale song calls and D-calls, b) zooplankton backscatter, c) tidal amplitude, and d) meridional and zonal wind stress were examined visually for seasonal trends. To examine submonthly timescales over the summer feeding season (January–June), wavelet transforms and wavelet coherence were applied; generalized linear models (GLM) were also applied. There was a 3-month lag between the seasonal onsets of high zooplankton backscatter (October) and blue whale acoustic presence (January), and an almost immediate drop in blue whale acoustic presence with the seasonal decrease of backscatter (June). This may be due to the use of memory by animals when timing their arrival on the feeding ground, but the timing of their departure may be related to detection of low prey availability. Over the summer feeding season, blue whale acoustic presence was strongly associated with zooplankton backscatter (GLM coefficient  $p \ll 0.0001$ ). Song calls followed a seasonal cycle, but D-calls appeared to respond to short term variations in environmental conditions over submonthly scales. Results suggest that spring tides may increase prey aggregation and/or transport into the Corcovado Gulf, leading to increased blue whale acoustic presence over 15-day or 30-day cycles; and short-lived events of increased wind stress with periodicities of 2–8 days and 16–30 days, may also contribute to the aggregation of prey. We discuss the strengths and limitations of coupling passive and active acoustic data to examine drivers of blue whale distribution.

\* Corresponding author.

E-mail address: [sbuchan@udec.cl](mailto:sbuchan@udec.cl) (S.J. Buchan).

<https://doi.org/10.1016/j.pocean.2021.102709>

Received 27 April 2021; Received in revised form 26 October 2021; Accepted 27 October 2021

Available online 2 November 2021

0079-6611/© 2021 The Authors.

Published by Elsevier Ltd.

This is an open access article under the CC BY-NC-ND license

(<http://creativecommons.org/licenses/by-nc-nd/4.0/>).

## 1. Introduction

Blue whales (*Balaenoptera musculus*) are the largest animals to have ever existed on Earth. They forage seasonally on highly productive mid- and high-latitude feeding grounds (e.g. Mackintosh and Wheeler, 1929; Huckle-Gaete et al., 2004; Croll et al., 2005). Blue whales have high energetic requirements, consuming 1–3 tons/day of euphausiids during their feeding season (Reilly et al., 2004; Goldbogen et al., 2011). They aggregate in areas where euphausiid density is predictably high (Croll et al., 2005; Hazen et al., 2015; Miller et al., 2019), where interannual environmental variability is low, and where long-term productivity is also high (Abrahms et al., 2019). Understanding the oceanographic drivers of blue whale presence on their feeding grounds is also a means of understanding the pelagic ecology and productivity of these marine ecosystems and developing strategies for species and habitat conservation (e.g. Palacios et al., 2013). In effect, marine mammals have been proposed as ecosystem sentinels (Moore, 2008; Hazen et al., 2019) given how their distributions respond to temporal changes in physical and biological oceanographic conditions over a range of temporal and spatial scales (e.g. Burtenshaw et al., 2004; Croll et al., 2005; Moore, 2008; Calambokidis et al., 2009; Stafford et al., 2018; Barlow et al., 2020; Pérez-Jorge et al., 2020).

Off the coast of Chile, a seasonal blue whale feeding ground in Northern Chilean Patagonia (NCP) (Huckle-Gaete et al., 2004, 2018; Buchan and Quiñones, 2016; Galletti-Vernazzani et al., 2012, 2017; Bedriñana-Romano et al., 2018, 2021) provides an accessible study site for examining the temporal variation of blue whale acoustic presence, zooplankton backscatter, and other atmospheric and oceanographic conditions. Between 570 (95% CI 475–705) and 762 (95% CI 638–933) blue whales use this feeding ground during the austral summer and autumn, based on photo-identification data (Galletti-Vernazzani et al., 2017). These whales feed predominantly on *Euphausia vallentini* (Buchan and Quiñones, 2016), which has in turn been proposed as a key species of the Chilean fjords and channels (Hamame and Antezana, 2010) and is an important prey item for commercially important fish species (Neira et al., 2015).

In the NCP mega-estuarine system, pelagic productivity is thought to be driven by (1) subantarctic water inputs from the Pacific Ocean and largely seasonal freshwater inputs from the continent (Dávila et al., 2002; Sievers and Silva, 2008), (2) highly seasonal variation in sunlight which drives primary production (Iriarte et al., 2007; González et al., 2011; Montero et al., 2011; Jacob et al., 2014) and (3) secondary production, including *E. vallentini* abundance (González et al., 2010; González et al., 2011; Buchan and Quiñones, 2016). Variation on a submonthly scale (i.e. several days to <1 month) has been described in NCP and is caused by wind-driven mixing events that increase primary production (Pérez-Santos et al., 2019), however this is not a system where productivity is primarily driven by wind-driven coastal upwelling. Over shorter timescales (hours to a day), semi-diurnal tides (Castro et al., 2011) and turbulent mixing and hypoxia (Pérez-Santos et al., 2018) cause changes in zooplankton abundance; and the diel vertical migration (DVM) behavior of zooplankton leads to changes in vertical distribution over 24-h cycles (Valle-Levinson et al., 2014; Pérez-Santos et al., 2018). Blue whale occurrence in NCP most likely responds to these temporal changes in the oceanographic processes which modulate prey abundance and patchiness over seasonal and submonthly timescales.

Blue whales produce loud song (sounds in repetitive patterned phrases) and non-song calls throughout their migratory range; therefore, acoustic detections can be used as an indicator of their presence (e.g. Stafford et al., 1999; Stafford et al., 2009; Buchan et al., 2014; Romagosa et al., 2020), with the limitation that silent animals cannot be detected by this method. The Southeast Pacific (SEP) blue whales present in NCP can be monitored acoustically using their highly stereotyped regional song dialect, known as “Southeast Pacific 2” or “SEP2” (Buchan et al., 2014, 2015). In addition to regional song calls, blue whales also produce non-regionally distinct highly variable downswept calls or “D-calls”

(Thompson et al., 1996). In blue whales, these long-range songs are produced by males and are thought to serve some reproductive function, while D-calls are thought to be short-range social calls produced by both males and females when animals are in close proximity (Lewis et al., 2018) and have been reported during a range of behaviors including feeding (Oleson et al., 2007a, 2007b; Lewis et al., 2018) and possible reproductive behaviors (Schall et al., 2020).

The only method that presently allows the collection of continuous data on whale presence over timescales of minutes to decades is passive acoustic monitoring (PAM) via the use of ocean bottom-mounted hydrophones (e.g. Van Parijs et al., 2009; Clark et al., 2015). However, the automated detection and classification methods used on these large datasets are not without error (Au and Lammers, 2016). Likewise, the use of hydroacoustic (or active acoustic) instruments, like echosounders or Acoustic Doppler Current Profilers (ADCPs), are the only means of collecting continuous acoustic backscatter data on the zooplanktonic prey of whales over comparable timescales (e.g. Nicol and Brierley, 2010; Širović and Hildebrand, 2011; Bozzano et al., 2014; Tsujii et al., 2016). However, most often PAM studies are carried out without simultaneously collecting backscatter data (notable exceptions include Širović and Hildebrand 2011; Baumgartner et al., 2014; Tsujii et al., 2016; Szesciorka et al., 2020). The inclusion of *in situ* oceanographic and/or backscatter greatly enhances the ability to answer questions about the environmental drivers of prey and whale distribution and/or behavior.

Seasonal variation in the acoustic presence of blue whale calls has been widely reported for feeding grounds worldwide (e.g. Stafford et al., 2001, 2009; Burtenshaw et al., 2004; Širović et al., 2004; Oleson et al., 2007b; Gavrilov and McCauley, 2013; Samaran, 2019; Leroy et al., 2018; Oestreich et al., 2020), and also in NCP (Buchan et al., 2015). Environmental drivers of this seasonal pattern have been examined in the North Pacific and the Southern Ocean with remotely-sensed oceanographic data, finding correlations between acoustic presence and sea surface temperature (Burtenshaw et al., 2004; Stafford et al., 2009), chlorophyll (Burtenshaw et al., 2004) and sea ice cover (Širović et al., 2004) given the effects of these variables on euphausiid prey. In NCP, we would expect seasonal changes zooplankton backscatter to be related to seasonal variation in blue whale acoustic presence. At the submonthly scale, variation in blue whale acoustic presence has only been examined in one recent study by Barlow et al. (2021) looking at intraseasonal variation and lags between sea surface temperature and wind stress variation and blue whale acoustic presence. In NCP, because zooplankton backscatter has shown variation over submonthly timescales due to low- and high-pressure atmospheric systems that drive variations in wind stress (Montero et al., 2017; Pérez-Santos et al., 2019), we expect processes that modulate euphausiid aggregation, like wind stress or tides, to be related to blue whale acoustic presence over submonthly timescales.

In this study, we ask: What drives blue whale acoustic presence on the NCP mega-estuarine feeding ground over time? This study couples PAM and hydroacoustic time series data with auxiliary oceanographic and meteorological data, to examine the temporal variation in blue whale acoustic presence and zooplankton backscatter over seasonal and submonthly scales.

## 2. Materials and methods

### 2.1. Study area and sampling approach

In this study, PAM data were used to examine the seasonal and submonthly variation in the acoustic presence of blue whale SEP2 song and D-calls. Here, acoustic presence was assumed to be an indicator of the presence of animals in the study area. Although this is a standard assumption in PAM studies of cetaceans (e.g. Stafford et al., 2009; Buchan et al., 2015; Romagosa et al., 2020), its shortcoming is that animals may be present in the study area but silent. Moreover, there is

currently no information globally on how sound production in individual blue whales changes over timescales greater than a few days, although recent studies of tagged blue whales off California reported higher sound production rates in autumn compared to summer (Lewis et al., 2018) and seasonal changes in diel calling behaviour (Oestreich et al., 2020). Here, zooplankton backscatter and oceanographic observations were examined as possible explanations for the seasonal and submonthly variation in blue whale acoustic presence in the NCP blue whale feeding ground.

An oceanographic mooring was deployed at 43° 51.96'S, 73° 31.28'W in the Corcovado Gulf (Fig. 1a) at a water depth of 162 m between January 2016 and February 2017. The mooring location consists of a quasi-enclosed basin to the northeast of Ascension Island (and port of Melinka) that is surrounded by subsurface shallow rises and islands and which communicates to the large Corcovado Gulf by deeper channels. The mooring was equipped with a hydrophone for collecting PAM data and an ADCP for collecting zooplankton backscatter data (Fig. 1b). Seasonal sampling cruises were conducted every 3 months to collect the following oceanographic data at the mooring site: stratified zooplankton net samples to validate the ADCP backscatter data, water column nutrient samples, and hydrological data (i.e., vertical profiles and horizontal cross-sections of temperature, salinity, oxygen and chlorophyll fluorescence, which is an indicator of phytoplankton biomass). Additional meteorological data (wind speed and direction) were also collected continuously at the nearby port of Melinka (Fig. 1a). Table 1 shows the temporal coverage of all data sets.

## 2.2. Passive acoustic monitoring data collection and processing

Passive acoustic monitoring data were collected using a Wildlife Acoustics SM3M Deep Water Songmeter hydrophone deployed at 140 m depth on the mooring line. Data were recorded continuously at a sample rate of 4 kHz and stored in 30 min files in .wav format. The collected acoustic files were analyzed to detect the occurrence of SEP2 blue whale song phrases (Fig. 2a) and D-calls (Fig. 2b). SEP2 songs were detected automatically via spectrogram cross-correlation using XBAT (Extensible Bioacoustic Tool; Bioacoustics Research Program 2012) with a data template of the C-D units of the SEP2 song phrase (as per Buchan et al., 2015) set at a detection threshold of 0.5, i.e. all detections with a

correlation score of  $\geq 0.5$  were included in the analysis. Spectrogram parameters were a fast Fourier transform (FFT) of 4096 samples, 25% overlap, and Hanning window. All detections were reviewed by an experienced analyst (LG) to remove false positives (incorrect detections). A 2% subsample of audio files from the entire acoustic dataset was reviewed manually by an experienced analyst (LG) and manually annotated and counted calls were used as a ground truth for comparison with the automatic detections to assess false negatives (missed calls). When comparing number of annotated calls with number of detected calls, the false negative rate was 8.36%.

PAM data were also analyzed for the occurrence of blue whale D-calls (Thompson et al. 1996; Schall et al., 2020) using the Low Frequency Detection and Classification System (LFDCS) (Baumgartner and Mussoline, 2011). Because D-calls are highly variable signals, spectrogram cross-correlation can generate high sources of error. The LFDCS detects sounds via pitch-tracking, extracts attributes of the pitch tracks (i.e., duration, frequency, time-frequency slope) and classifies the sounds by comparing their attributes to those of each call type in an a-priori constructed call library using quadratic discriminant function analysis. The Mahalanobis distance (MDist) of each pitch track provides a measure of how well the attributes of an unknown sound match the multivariate distribution of attributes for a call type in the call library; the MDist can therefore be used as a detection threshold (Baumgartner et al., 2013, 2014; Davis et al., 2017). A call library of three variants of the D-call was developed in LFDCS based on a total of 1222 exemplars classified by experienced analysts (CR and LG). Only D-calls classified with an MDist  $\leq 5$  were counted as detected events. To further reduce false positives, post-processing filters were applied where only detections of  $>0.4$  s duration,  $>3$  Hz bandwidth and  $>3$  detections per hour of data were considered in the analysis. These detections were checked manually and validated as true or false detections; all false detections were removed from the time series (achieving 0 false positives). To assess the false negative rate, a 2% subsample of the audio files from the data was reviewed manually by an analyst (LG) and manual annotations of calls were used as a ground truth to compare with the automatic post-processed call detections. The false negative rate was 41.74%.

The start date and time of all SEP2 and D-call detections were compiled as a time series. To examine seasonal and submonthly temporal occurrence and variation, daily detections were plotted over the

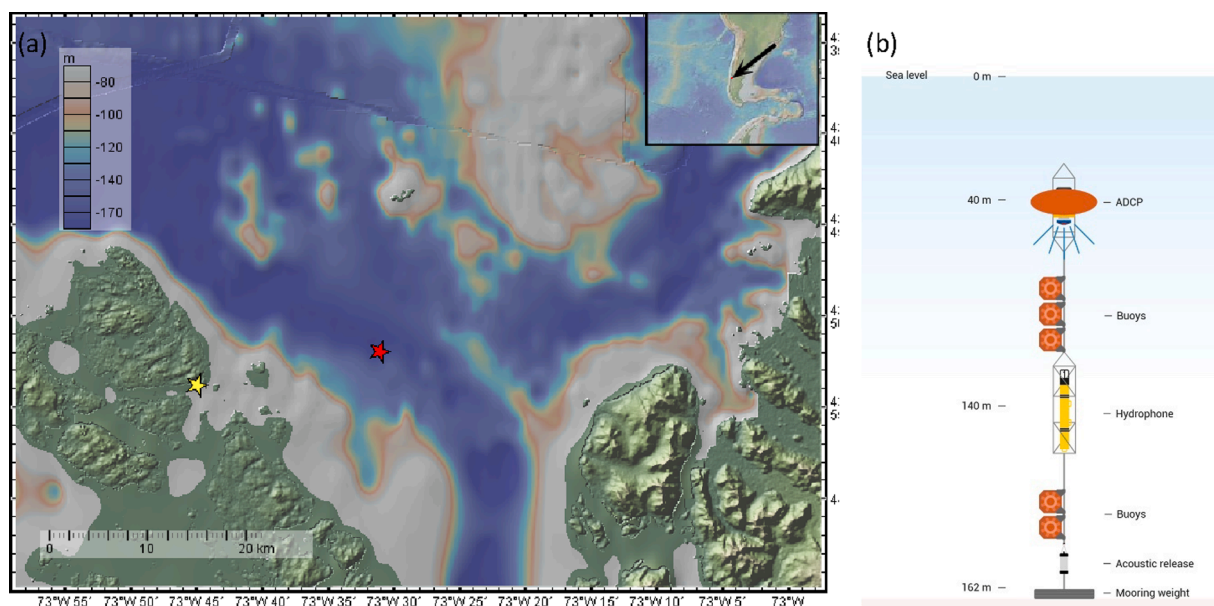


**Fig. 1.** (a) Bathymetric map of Corcovado Gulf study area with the geographical position of the oceanographic mooring (red star) and the meteorological station (yellow star). (b) Schematic of oceanographic mooring design with hydrophone at the 140 m depth and a downward-facing Acoustic Doppler Current Profiler at 40 m.

**Table 1**

Temporal coverage of data collection in the Corcovado Gulf and port of Melinka (for meteorological data only). Start or end dates of time series and *in situ* sampling dates shown in parentheses.

Date type	Jan 2016	Feb 2016	Mar 2016	Apr 2016	May 2016	Jun 2016	Jul 2016	Aug 2016	Sep 2016	Oct 2016	Nov 2016	Dec 2016	Jan 2017	Feb 2017
Passive acoustic monitoring time series	● (8th)	●	●	●	●	●	●	●	●	●	●	●	●	● (7th)
ADCP backscatter time series	● (8th)	●	●	●	●	●	●	●	●	●	● (15th)			
Zooplankton sampling								● (2nd)			● (17th)			
Nutrient sampling	● (8th)			● (10th)				● (2nd)			● (17th)			
Hydrological (temperature, salinity, and fluorescence) profiles and cross-sections	● (8th)			● (10th)				● (2nd)			● (17th)			
Meteorological time series	● (8th)	●	●	●	●	●	●	●	●	●	● (17th)			

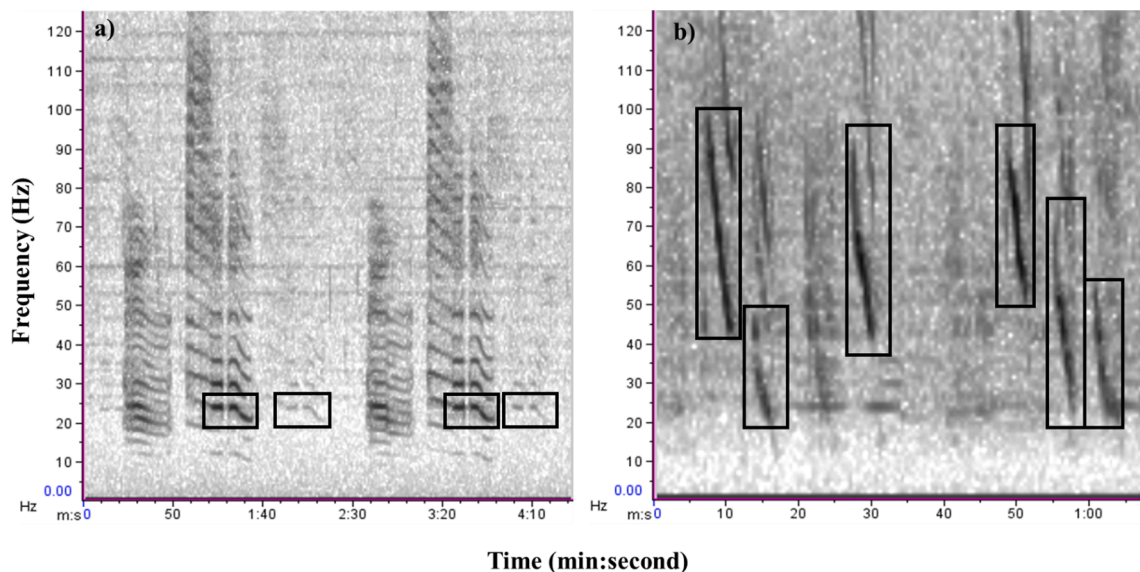


**Fig. 2.** Spectrograms of (a) two complete phrases of Southeast Pacific 2 (SEP2) blue whale song calls. Spectrogram parameters: FFT: 8192 samples, 50% overlap, Hann Window; and (b) blue whale D-calls recorded in this study. Spectrogram parameters: FFT: 4096 samples, 50% overlap, Hann Window. Boxes show the unit(s) identified by automatic detectors.

entire study period and a wavelet analysis was applied to the data (see Section 2.7 for methods of wavelet analysis).

### 2.3. Hydrophone detection range estimation

Because blue whale vocalizations are very high amplitude and low frequency, these sounds can propagate over large distances, sometimes up to several hundreds of km (e.g. Sirović et al., 2007). Therefore, calls detected at a hydrophone may originate from animals far from the hydrophone. In contrast, ADCP backscatter measurements, and other mooring-based oceanographic sampling are representative of a single point in space. Therefore, estimating the detection range of the hydrophone is fundamental to be able to compare the spatial scales of PAM and that of the backscatter data. The detection range of blue whale song calls at the hydrophone was estimated using (a) the Passive Sonar Equation (Urlick, 1975) to determine the maximum transmission loss ( $TL_{max}$ , in dB) before a blue whale song call becomes undetectable i.e. falls below a certain signal to noise ratio (SNR), and (b) the Range-dependent Acoustic Model (RAM) (Collins, 1993) which models Transmission Loss (TL) over range (km) at the study site, based on the sound speed conditions and the bathymetry along an azimuth from the mooring. Detection range is therefore estimated from the RAM output as

the distance at which  $TL = TL_{max}$ .

The Passive Sonar Equation was used to calculate  $TL_{max}$  (where  $TL = SL - NL - SNR$ ). Blue whale song Source Level (SL) was assumed at 174 dB re: 1μPa at 1 m over 17–50 Hz based on estimations for pygmy blue whales in the Indian Ocean by Samaran et al. (2010a). Southeast Pacific blue whales are on average less than 1 m larger than pygmy blue whales (Pastene et al., 2020), so given the lack of source level estimation for SEP blue whales, a pygmy blue whale source level was used for song notes. Blue whale D-call source levels have been reported as 155–166 dB re: 1μPa at 1 m over 38–88 Hz in the Atlantic (Berchok et al., 2006), so we assumed 166 dB re: 1μPa at 50 Hz. Ambient noise levels (NL) for April in the 1/3 octave band centered at 25 Hz were 86.2 dB re: 1μPa, and 85.8 dB in the 1/3 octave band centered at 50 Hz, as determined by calculating levels averaged the month using PAMGuide (Merchant et al., 2015). Hydrophone sensitivity of  $-164.1$  dB re 1 V/μPa and a recorder sensitivity of 0 gain were provided for the hydrophone by Wildlife Acoustics. A conservative SNR of 10 dB was assumed. Therefore, transmission loss had to be less than 77.8 dB for songs to be detected and 70.2 dB for the loudest D-calls. The RAM was implemented in MATLAB. The model assumptions and inputs were: The calling whale was assumed to produce sound at 20 m depth at the SL mentioned above at a frequency of 23.6 Hz for SEP2 blue whale song and 50 Hz for D-calls

(Buchan et al., 2015; Patris et al., 2019; Oleson et al., 2007a; Lewis et al., 2018). The hydrophone (receiver) depth was set at 140 m, with total water column depth of 162 m. Sound Speed Profiles (SSP) were calculated using the *in situ* temperature and salinity data collected in April (autumn) (see Section 2.9). Bathymetric cross-section data from 30° radian azimuths were downloaded from <https://www.gmrt.org/GMRTMapTool/> and extracted in MATLAB. Sediment type was assumed to be sand based on anecdotal reports from fishermen. Detection ranges were calculated for each bathymetric cross-section and the distance at which TL was >78 dB or 70 dB for song and D-calls respectively.

#### 2.4. ADCP backscatter data collection and processing

Volume backscatter strength (Sv, in dB re m<sup>-1</sup>) derived from ADCP data is widely used to study the relative abundance and distribution of zooplankton (e.g. Brierley et al., 2006; Baumgartner and Fratantoni, 2008; Nicol and Brierley, 2010; Valle-Levinson et al., 2014; Pérez-Santos et al., 2018). Backscatter data were obtained from a Teledyne RDI Workhorse ADCP with a single-frequency echosounder of 307.7 kHz. The ADCP was deployed at 40 m depth and pointed downwards, capturing echo intensity data from depths of approximately 45 m to the bottom i.e. 140 m. Data were collected hourly with a vertical bin size of 1 m. The ping interval was 240 ping per hour, i.e. 1 ping every 15 s from which an hourly average was calculated.

The ADCP echo intensity was converted to mean volume backscatter strength (Sv, in dB re 1 m<sup>-1</sup>) following Eq. (1):

$$S_v = C + 10 \log [(T_x + 273.16)R^2] - L_{DBW} - P_{DBW} + 2\alpha R + K_c(E - E_r) \quad (1)$$

where  $C$  is a sonar-configuration scaling factor (-148.2 dB for the Workhorse Sentinel),  $T_x$  is the temperature at the transducer (°C),  $L_{DBW}$  is  $\log_{10}$ (transmit pulse length = 8.13 m),  $P_{DBW}$  is  $\log_{10}$ (output power = 15.5 W),  $\alpha$  is the absorption coefficient (dB m<sup>-1</sup>),  $K_c$  is a beam-specific sensitivity coefficient (supplied by the manufacturer as 0.45),  $E$  is the recorded AGC (automatic gain control), and  $E_r$  is the minimum AGC recorded. The beam average of the AGC for the 4 transducers was used to obtain optimal results following the procedure in Brierley et al. (2006). Finally,  $R$  is the slant range to the sample bin (m), which uses the vertical depth as a correction (Lee et al., 2004). Therefore,  $R$  is expressed as Eq. (2),

$$R = \frac{b + \frac{L+d}{2} + ((n-1)d) + \left(\frac{d}{4}\right) \bar{c}}{\cos \zeta} \frac{\bar{c}}{c_t} \quad (2)$$

where  $b$  is the blanking distance (3.23 m),  $L$  is the transmit pulse length (8.13 m),  $d$  is the length of the depth cell (1 m),  $n$  is the depth cell number of the particular scattering layer being measured,  $\zeta$  is the beam angle (20°),  $\bar{c}$  is the average sound speed from the transducer to the depth cell (1,453 m s<sup>-1</sup>) and  $c_t$  is the nominal sound speed used by the instrument (1,454 m s<sup>-1</sup>).

Volume backscatter strength (Sv) was converted to the volume backscattering coefficient (sv) (Eq. (3)); sv was integrated over the water column between 45 m (z1) and 140 m (z2) to obtain the area backscattering coefficient (sa) (Eq. (4)), and then converted to area backscattering strength (Sa, dB re 1(m<sup>2</sup> m<sup>-2</sup>)) (Eq. (5)) (MacLennan et al., 2002). Volume backscatter strength (Sv) was also processed as time series at 50 m and at 100 m.

$$s_v = 10^{(S_v/10)} \quad (3)$$

$$s_a = \int_{z_1}^{z_2} s_v dz \quad (4)$$

$$S_a = 10 \log_{10}(s_a) \quad (5)$$

*In situ* samples of zooplankton were collected to validate the

backscatter signal in winter and spring; logistical constraints meant that better coverage was not possible. The primary interest in this study is the *meso*-zooplankton since this is the size fraction that contains euphausiids, which are known blue whale prey (Reilly et al., 2004; Croll et al., 2005; Goldbogen et al., 2011). Net sampling was carried out twice, in August at the same time as ADCP data were being collected and in November, two days after the ADCP was recovered due to logistical difficulties of sampling on the same day. Stratified zooplankton net sampling was carried out using a Tucker trawl net with a 0.25 m<sup>2</sup> mouth opening and a 300 μm mesh net equipped with a flowmeter to quantify the volume of water sampled. Oblique tows integrated over the following four depth strata: 0–25 m, 25–50 m, 50–100 m and 100–150 m. Samples were preserved in buffered formaldehyde (5%) and stored for later analysis. In the laboratory, organisms were measured (length) and sorted into size-classes using a 5 mm length threshold (*meso*-zooplankton); and then sorted into functional groups and counted (individuals m<sup>-3</sup>). Based on abundance (individuals-m<sup>-3</sup>), biomass (μg dry weight m<sup>-3</sup>) was also estimated for chitinous zooplankton groups larger than 5 mm length at each sampling depth. Estimates for these groups were based on the available average reported dry weight of one of the most common copepods in the Humboldt Current, *Calanus chilensis* of 2.5 mm prosome length (PL) and 115.6 μg dry weight (Giraldo et al., 2002). Assuming cylindrical body shape, the average size of the most common species found within each chitinous group were converted from length to biomass for: large copepods (*Rhincalanus nasutus*), PL 5.1 mm; euphausiids (*E. vallentini*), Total Length (TL) 14 mm; amphipods (possibly *Themisto gaudichaudi*), TL 7 mm; and zoea (possibly *Nauticaris magellanica*), PL = 5.8 mm.

#### 2.5. Meteorological data collection and processing

Data from the meteorological station at Melinka (Fig. 1b, 43° 53' 48.80"S, 73° 44' 57.44"W) were used to examine seasonal and sub-monthly variability in the atmospheric forcing regime during the sampling period. Wind data were used to calculate zonal ( $\tau_u$ ) and meridional ( $\tau_v$ ) wind stress:

$$\tau_u = \rho_a C_d u_{10} U_{10}, \quad \tau_v = \rho_a C_d v_{10} U_{10} \quad (6)$$

where  $\rho_a$  is air density (1.2 kg m<sup>-3</sup>),  $C_d$  is a dimensionless drag coefficient,  $u_{10}$  and  $v_{10}$  are the zonal and meridional wind components, respectively, and  $U_{10}$  is the magnitude of the wind vector 10 m above sea level.

The drag coefficient was calculated using the formula proposed by Yelland and Taylor, 1996) in which the coefficient varies as a function of wind speed. The average wind speed was 2.9 m s<sup>-1</sup>, with an absolute maximum of 11.1 m s<sup>-1</sup>.

$$C_d = 0.29 + \frac{3.1}{U_{10}} + \frac{7.7}{U_{10}^2} \times 10^{-3}, \quad \text{for } U_{10} \leq 6 \text{ms}^{-1} \quad (7)$$

$$C_d = 0.60 + 0.070 U_{10} \times 10^{-3} \quad \text{for } 6 \text{ms}^{-1} \leq U_{10} \leq 26 \text{ms}^{-1} \quad (8)$$

#### 2.6. Tidal amplitude data processing

Tidal current amplitude and tidal elevation amplitude were obtained by first high-pass filtering one of the ADCP east-velocity bins and the tides record to eliminate subtidal variations. The high-pass filtered signals were then subject to complex demodulation (e.g. Thompson and Emery, 2014) to the semidiurnal band, thus providing periods of spring and neap tides.

#### 2.7. Wavelet analyses

Seasonal trends were described based on visual examination of time series and using Generalized Linear Models (GLMs); variation over submonthly timescales were examined using wavelet analyses. Only

months with acoustic presence of blue whales were included in these analyses, i.e. January to June (see Results), considered to be the months of the 6-month feeding season. For these analysis, passive and active acoustics, and wind stress time series were processed into daily values to examine their temporal scales of variation over seasonal and sub-monthly timescales. The PAM data were processed into a time series of daily detections (SEP2 song call and D-calls). Acoustic Doppler Current Profiler backscatter data were processed into daily time bins of integrated backscatter (Sa) and Sv at 50 m and 100 m.

Wavelet transforms (Torrence and Compo, 1998) using the Morlet wavelet limited to 32 days was applied to the daily song call and D-call time series (daily call counts), the daily Sv (50 m and 100 m) and Sa time series, the meridional and zonal wind stress time series, and tidal amplitude. The wavelet transform reveals dominant significant (at 95% confidence) periodicities of time series and when these periodicities are most energetic over time.

## 2.8. Generalized linear models and wavelet coherence

To test the hypothesis that blue whale submonthly acoustic presence is related to zooplankton backscatter, tide amplitude or wind stress over the 6-month summer feeding season, GLMs with a binomial link function were fitted in R (R Core Team, 2019) for daily blue whale acoustic presence as the response variable, and either integrated backscatter (Sa) over 45–140 m, Sv at 50 m, Sv at 100 m, tidal amplitude, or wind stress (zonal or meridional) as explanatory variables. Models were fitted with only one variable at a time to test these specific hypotheses. Daily blue whale acoustic presence was determined as any day with 1 or more calls (either SEP2 or D-call), which was assigned a score of 1; days with no calls were assigned a score of 0. The same was done for song call presence only and D-call presence only. Coefficients of each variable were examined for significance to test hypotheses (at  $p \leq 0.05$ ), and the predicted response curves were examined to determine the nature of the relationship. Thus, a positive response curve and a significant coefficient would support the hypothesis that acoustic presence is associated with increasing levels of the explanatory variable (backscatter, wind stress or tidal amplitude). The Akaike information coefficient was also calculated for all GLMs to examine which model(s) had the best fit, where a small Akaike information coefficient indicates a better fitting model.

Wind stress was found to be non-significant over the summer feeding season (see Results), so in order to examine any effects at shorter timescales (<1 month), wavelet coherence was calculated, which is a measure of correlation (magnitude-squared coherence) between two wavelet time series at specific periods. Since no submonthly signal was detected in the wavelet time series for song calls, wavelet coherence was only applied to comparisons of D-calls to meridional and zonal wind stress.

## 2.9. Hydrographic profiles and cross-sections

Seasonal hydrographic profiles were obtained with a temperature, conductivity and depth (CTD) instrument (Seabird 25), with additional dissolved oxygen (DO) (SBE 43) and fluorescence (Wet Labs Wet Star) sensors sampling at 8 Hz with a descent rate of  $\sim 1 \text{ m s}^{-1}$ . The data, which had a nominal vertical resolution of  $\sim 12 \text{ cm}$ , were averaged into 1 m bins following the manufacturer's recommendations. The conservative temperature (C) and absolute salinity ( $\text{g kg}^{-1}$ ) were calculated according to the Thermodynamic Equation of Seawater 2010 (IOC SCOR, 2010). Cross-section profiles were taken at 7 stations over a 15 km transect between the mooring site and the nearest land mass. Using the CTD data, water mass classification was carried out based on Sievers (2008) and Sievers and Silva (2008).

Nutrient profiling at the mooring site was done by collecting water samples at various depths (0 m, 5 m, 10 m, 25 m, 50 m, 75 m, 100 m, 125 m, 150 m) with Niskin bottles. Water samples were analyzed spectrophotometrically following the standard methods of Strickland

and Parsons (1968) to determine inorganic nutrients (nitrite, nitrate, phosphate and silicic acid).

## 3. Results

### 3.1. Temporal variation in blue whale song calls and D-calls

Both blue whale SEP2 song calls (Fig. 2a) and D-calls (Fig. 2b) were detected in the PAM data. Overall, song call detections ( $n = 35,729$ ) were six times higher than D-calls ( $n = 6,199$ ) (Fig. 3a), however it is important to bear in mind that the false negative rate for the detection of individual D-calls was 41.74% compared with 8.36% for the song detector, so many more D-calls were missed by automatic detector than song calls. Correcting with this false negative rate would indicate about 10,000 D-calls.

The detection range of blue whale song calls from the mooring location was estimated between 2.75 km and 15.3 km depending upon the azimuth of choice, i.e. the bearing of the whale relative to the hydrophone, with an overall listening area of  $250 \text{ km}^2$  (see Supplementary Materials Fig. 1). The detection range of D-calls for the mooring location was estimated to be 1.4 km to a maximum of 6 km, depending upon the azimuth. For both call types, detection ranges to the southwest of the hydrophone were shortest. The reduced detection range of D-calls as compared to song calls suggests that over the same area, D-call density may be higher at times than that of song calls.

Blue whale calls were largely present between January 2016 and June 2016 (Fig. 3a), so for the purposes of wavelet and statistical analyses, the summer feeding season was defined as January to June. Song calls were heard between January 2016 and July 2016, and again in January 2017 until the end of the time series in February 2017. D-calls were present January-May 2016 and December 2016 through to the end of the time series. There was with a strong seasonal peak in song calls between March 2016 and June 2016, however no clear seasonal peak was found for D-calls; instead, two main peaks in D-calls were observed: one at the end of March/beginning of April 2016 and one in May 2016.

The wavelet analysis over the summer feeding season (January to June) revealed significant periodicities that fluctuated between 1 and 7 days and 12–32 days for D-calls, but no significant periodicities were detected for song calls (Fig. 4a,b).

### 3.2. Temporal variation in ADCP backscatter time series

The integrated backscatter (Sa) over 45–140 m time series showed seasonally high zooplankton backscatter between January and June 2016, and October and November 2016, when the time series ended (Fig. 3b). Integrated backscatter was less intense in winter (July–September). This indicates a seasonal cycle where backscatter increases in the austral spring and remains high until late summer.

During the feeding season, Sv at 50 m was mostly higher than Sv at 100 m. During the winter, backscatter at 100 m exceeded backscatter at 50 m. Within the summer feeding season, two peaks in backscatter (50 m, 100 m and Sa) were observed: at the end of March/beginning of April and in May. Integrated backscatter also displayed a very strong peak in February (Fig. 3b). From the wavelet analysis, significant periods of 10–24 days was found for water column integrated backscatter, backscatter at 50 m and backscatter at 100 m, although the latter was short lived (Fig. 4d,e).

From the stratified meso-zooplankton net sampling, the overall biomass of meso-zooplankton groups throughout the water column increased from the August sampling to November sampling (Fig. 5a), coinciding with the observed increase in backscatter between winter and spring (Fig. 3b). Euphausiids had the highest biomass of all groups, which doubled between winter (average  $2,379.1 \mu\text{g m}^{-3}$ ) and spring (average  $5,968.5 \mu\text{g m}^{-3}$ ). High backscatter values at depth during daylight hours (Fig. 5b,c) coincided with high biomass of euphausiids and amphipods (winter) and euphausiids and copepods (spring) in the

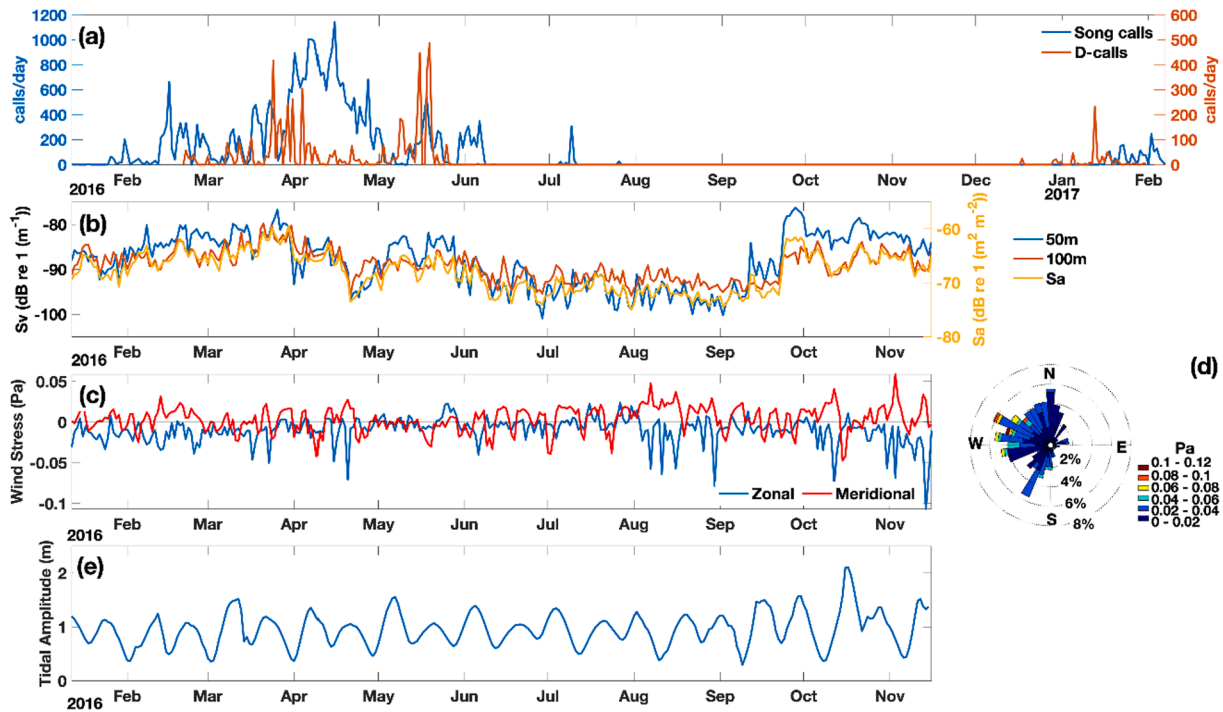


Fig. 3. Time series data for (a) Southeast Pacific blue whale song calls and D-calls. Note: No song calls were present between August and December 2016; no D-calls were present June and November 2016; (b) Volume backscattering strength ( $S_v$  in  $\text{dB re } 1 (\text{m}^{-1})$ ) calculated from the ADCP at 50 m and 100 m depth, and integrated backscatter between 45 m and 140 m ( $S_a$  in  $\text{dB re } 1 (\text{m}^2 \text{m}^{-2})$ ), (c) zonal (u) and meridional (v) wind stress (Pa); (d) wind rose diagram representing the wind stress (Pa) and direction between January and November 2016; (e) tidal amplitude (m).

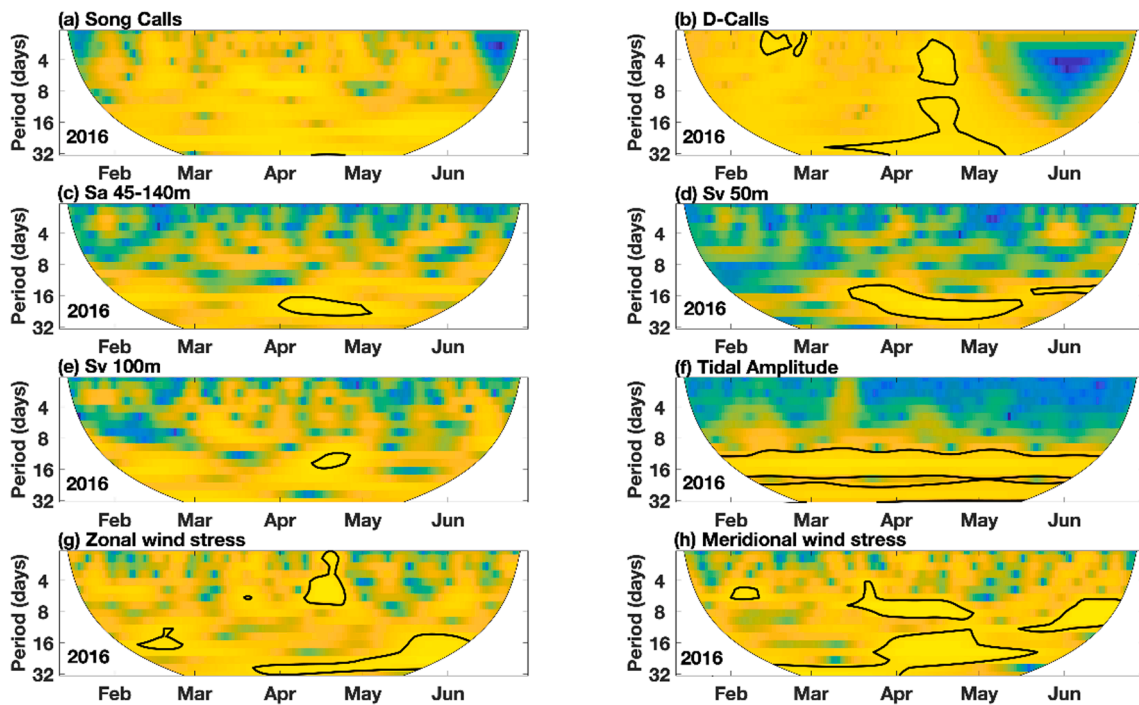
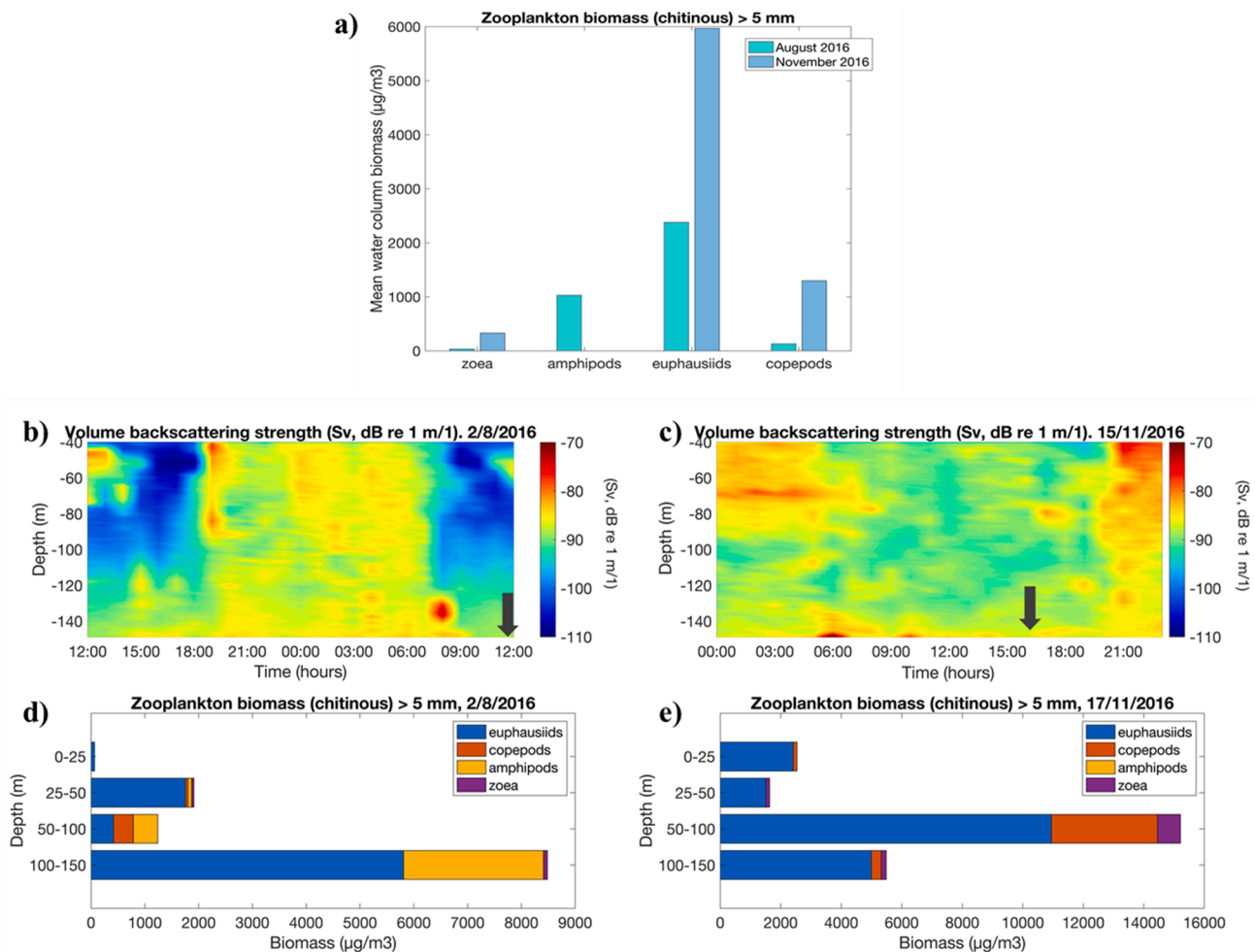


Fig. 4. Wavelet analysis of periodicities (days) for time series between January and June 2016 for (a) Southeast Pacific blue whale song calls and (b) D-calls; (c) Integrated backscatter ( $S_a$  in  $\text{dB re } 1 (\text{m}^{-1}) \text{m}$ ) over 45 m and 140 m, (d)  $S_v$  (in  $\text{dB re } \text{m}^{-1}$ ) measured at 50 m and (e) measured at 100 m; (f) tidal amplitude (m); and (g) zonal and (h) meridional wind stress (Pa). Significant periodicities of variation are shown within black lines.

two deepest sampling strata (100–150 m, 50–100 m) where zooplankton should be more abundant at certain times of the day (Fig. 5d,e). These results provide some validation of the backscatter data, suggesting that high backscatter at this site is due to high euphausiid abundance.

### 3.3. Temporal variation in wind stress and tidal amplitude

The annual time series of surface wind from Melinka showed a predominance of westerly winds, and pulses of northerly and southerly



**Fig. 5.** (a) Mean water column abundance ( $\text{ind.}/\text{m}^3$ ) of meso-zooplankton (>5mm length class) groups in the austral winter (August) and spring (November). Volume backscattering strength (Sv in dB,  $\text{re m}^{-1}$ ) between 45 m and 140 m depth in (b) winter and (c) spring. Note: The ADCP was removed on 15 November 2016 but the zooplankton sampling was carried out two days later due to logistical constraints. Arrows indicate the time of day of *in situ* zooplankton sampling on the 2nd of August and the time of day on 17 November 2016. Profiles of meso-zooplankton groups sampled from four depth strata (0–25 m; 25–50 m; 50–100 m; 100–150 m) during daylight hours in (d) winter and (e) spring.

winds stress (Fig. 3c,d). The wavelet analysis applied to wind stress showed submonthly periods between 2–8 days and 16–30 days for zonal wind stress (Fig. 4g), and between 4 and 32 days for meridional wind stress (Fig. 4h). Semidiurnal tidal amplitude variability responds to the fortnightly neap/spring tidal cycle (Fig. 3e), with significant periods around 15 and 30 days throughout the entire time series (Fig. 4f).

### 3.4. Generalized linear models and wavelet coherence

Predicted GLM response curves revealed a positive relationship between daily blue whale acoustic presence and daily averaged water column integrated backscatter (Fig. 6a), with highly significant coefficients for integrated backscatter, backscatter at 50 m and at 100 m ( $p < 0.0001$ ; Table 2; predicted response curves for the latter two not shown). Integrated backscatter also had highly significant coefficients when song call and D-call presence ( $p < 0.0001$ ) were set as response variables (Table 2; Fig. 6b,c). The predicted response curve for presence as a function of tidal amplitude was positive (Fig. 6d), with a significant coefficient ( $p < 0.05$ ; Table 2). No significant coefficients were found for zonal ( $p > 0.05$ ) and meridional ( $p > 0.05$ ) wind stress as explanatory variables, although response curves showed positive relationships (Fig. 6e,f). The GLM with the lowest Akaike information coefficient was for presence- integrated backscatter (Table 2).

Wavelet coherence between D-calls and meridional and zonal wind

stress showed short windows of moderate (>0.6 magnitude-squared coherence) and high (>0.8 magnitude-squared coherence) correlation over mainly periods of 4–8 days and 14–24 days, with highest correlations occurring in April and May (Fig. 7a,b).

### 3.5. Auxiliary hydrographic profiling and nutrient data

Seasonal cycles were observed in temperature, salinity, dissolved oxygen (DO) and chlorophyll fluorescence (Fig. 8). Warmer surface temperatures (14–16 °C) were observed during summer over the first 25 m of the water column (Fig. 8a). Temperature decreased from summer to winter, and then increased again in spring. Salinity revealed the influence of Estuarine Water (EW) only during the summer season, observed as a thin surface layer with salinity values ranging from 30 to 31 g/kg (Fig. 8e). At depth, Modified Subantarctic Water (MSAWW), Subantarctic Water (SAAW), and Equatorial Subsurface Water (ESSW) were identified during summer, autumn and spring; only SAAW was observed in winter in a well-mixed water column (Fig. 8f-h). In general, the first 100 m of the water column was well ventilated, especially during the winter season, where DO was between 4 and 5 mL/L (Fig. 8i-l). Lower values of DO at depth were measured in summer and autumn from 100 m to the bottom (Fig. 8i-l). Fluorescence only showed higher values in surface layers during summer and spring (Fig. 8m-p).

Inorganic nutrient profiles also indicated a seasonal pattern, showing



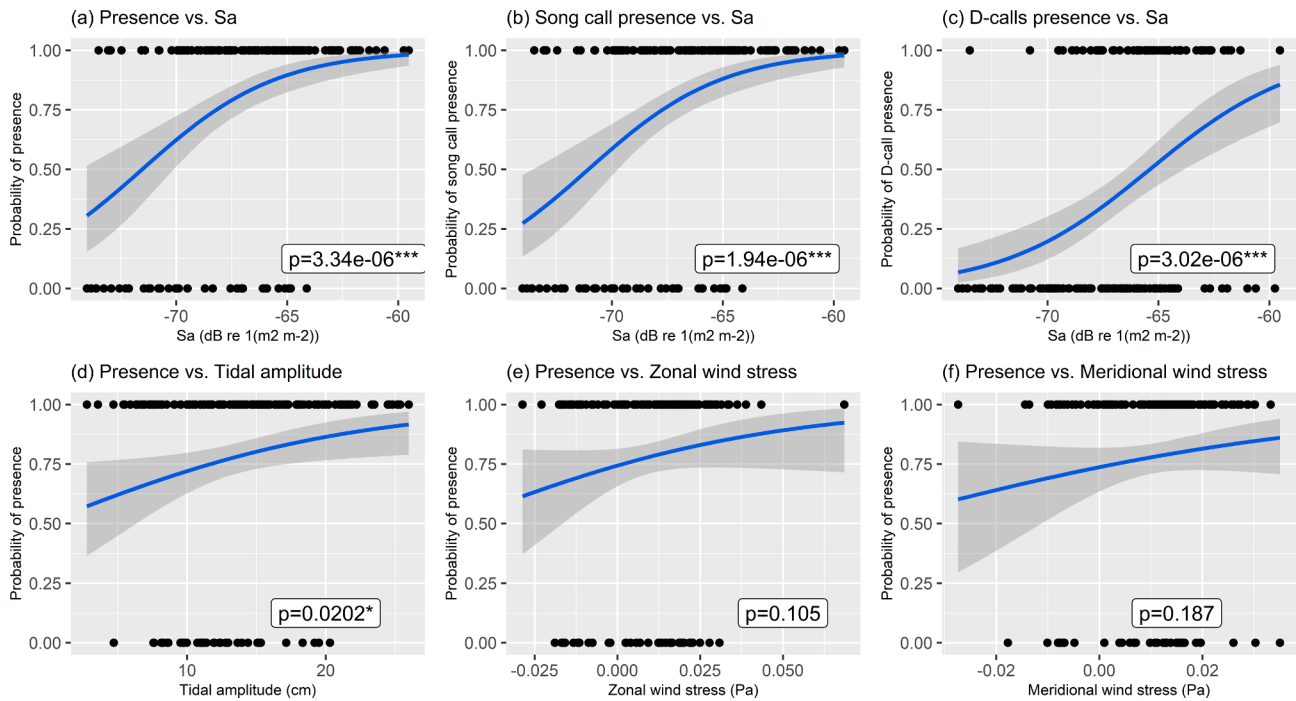


**Fig. 6.** Response curves (blue line) and 95% confidence intervals (grey shaded area) for generalized linear models (GLMs) of: (a) daily blue whale acoustic presence (song call + D-call) and integrated backscatter (Sa) over 45–140 m (dB re 1(m<sup>2</sup> m<sup>-2</sup>)), (b) song call presence and integrated backscatter (Sa) over 45–140 m (dB re 1(m<sup>2</sup> m<sup>-2</sup>)), (c) D-call presence and integrated backscatter (Sa) over 45–140 m (dB re 1(m<sup>2</sup> m<sup>-2</sup>)), (d) daily blue whale acoustic presence and tidal amplitude (cm), (e) zonal and (f) meridional wind stress (Pa). Inset boxes report coefficient values \*\* 0.05 > p > 0.001, \*\*\* p < 0.001.

**Table 2**

Summary table of Generalized Linear Models results, including the explanatory variable coefficient (coefficient values: \*\* 0.05 > p > 0.001, \*\*\* p < 0.001) and the Akaike information criteria.

Response variable	Explanatory Variable	Explanatory variable coefficient	Akaike information criterion
Presence	Integrated backscatter 45–140 m	3.34e-06	158.91
Presence	Backscatter at 50 m	8.03e-05***	167.84
Presence	Backscatter at 100 m	8.22e-06***	159.69
Song call presence	Integrated backscatter 45–140 m	1.94e-06 ***	166.89
D-call presence	Integrated backscatter 45–140 m	3.02e-06 ***	206.74
Presence	Tidal amplitude	0.0202*	179.36
Presence	Zonal wind stress	0.105	182.5
Presence	Meridional wind stress	0.187	183.43

the importance of the winter mixing in nitrate, phosphate, and silicic acid (Supplementary Materials Fig. 2). During January and November, lower values of nutrients were observed in the surface layer from seasonal phytoplankton uptake. In April, an increase at depth in nitrate and silicic acid was observed (Supplementary Materials Fig. 2).

#### 4. Discussion

##### 4.1. Seasonal variation in blue whale acoustic presence and prey backscatter

A clear pattern in seasonal acoustic presence was found, where blue whale song calls occurred between January and June (austral summer and autumn) with a seasonal peak around April. This seasonal trend is

consistent with a previous report by Buchan et al. (2015) in this study area. Summer and autumn blue whale acoustic presence has been reported for other feeding grounds, like the North Pacific (e.g. Stafford et al., 2001; Burtenshaw et al., 2004).

Based on the backscatter time series (integrated, 50 m and 100 m), seasonally high zooplankton biomass occurs between October (spring) and June (autumn) in NCP. Euphausiid biomass was found to increase two-fold between August (winter) and November (spring). When our limited net sampling effort is combined with previous observations in this area, it is reasonable to conclude that high euphausiid biomass is largely responsible for the high backscatter in spring, summer and autumn. The seasonal increase in backscatter that we observed coincides with reports by González et al. (2010) and Buchan and Quiñones (2016), who found that the mesozooplankton in the Corcovado Gulf was dominated by *E. vallentini* in the austral winter (July) and spring (November), with a marked increase in abundance between winter and spring/summer. Hydrographic data showed stratified surface layers and the appearance of Modified Subantarctic Water (MSAAW) in spring and summer, which is a water mass that has been found to boost primary productivity due to its high silicate content (Torres et al., 2014; Buchan and Quiñones, 2016). Increased nutrient concentrations in surface layers, probably due to winter mixing, were taken up during phytoplankton growth in spring. In spring and summer, nutrient levels dropped in surface layers (0–20 m), coinciding with high surface fluorescence in spring and summer due to phytoplankton growth (Supplementary Materials Fig. 2).

A three-month lag was observed between the onset of the seasonal increase in zooplankton backscatter (October 2016) and the detection of blue whales on their feeding ground (January 2017) (Fig. 3). The January arrival of blue whales on their feeding ground (this study and Buchan et al., 2015) may be timed to coincide with sufficient euphausiid biomass following several months of euphausiid growth during the austral spring (between October and December). This is consistent with findings by Bedriñana-Romano et al. (2018) who reported a two- to four-month lag between increased remotely-sensed chlorophyll-a

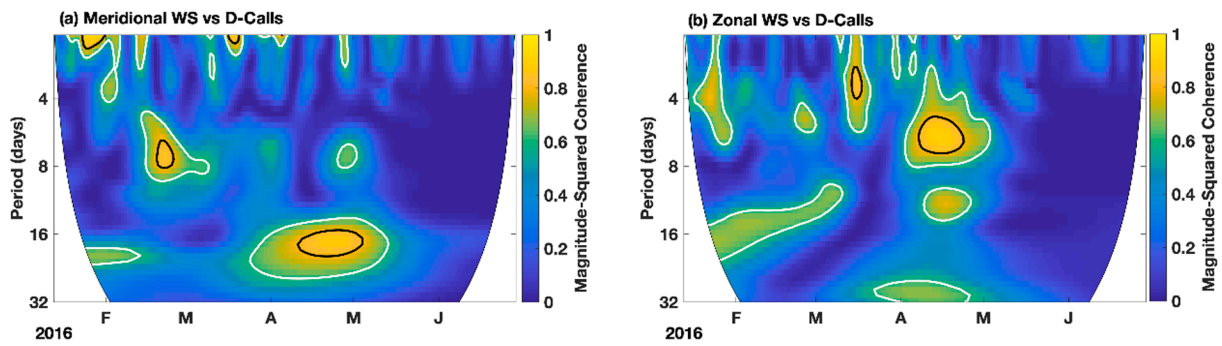


Fig. 7. Wavelet coherence analysis of (a) D-calls and meridional wind stress (Pa); (b) D-calls and zonal wind stress (Pa). White contour lines indicate > 0.6 magnitude-squared coherence and black contour lines indicate > 0.8 magnitude-squared coherence.

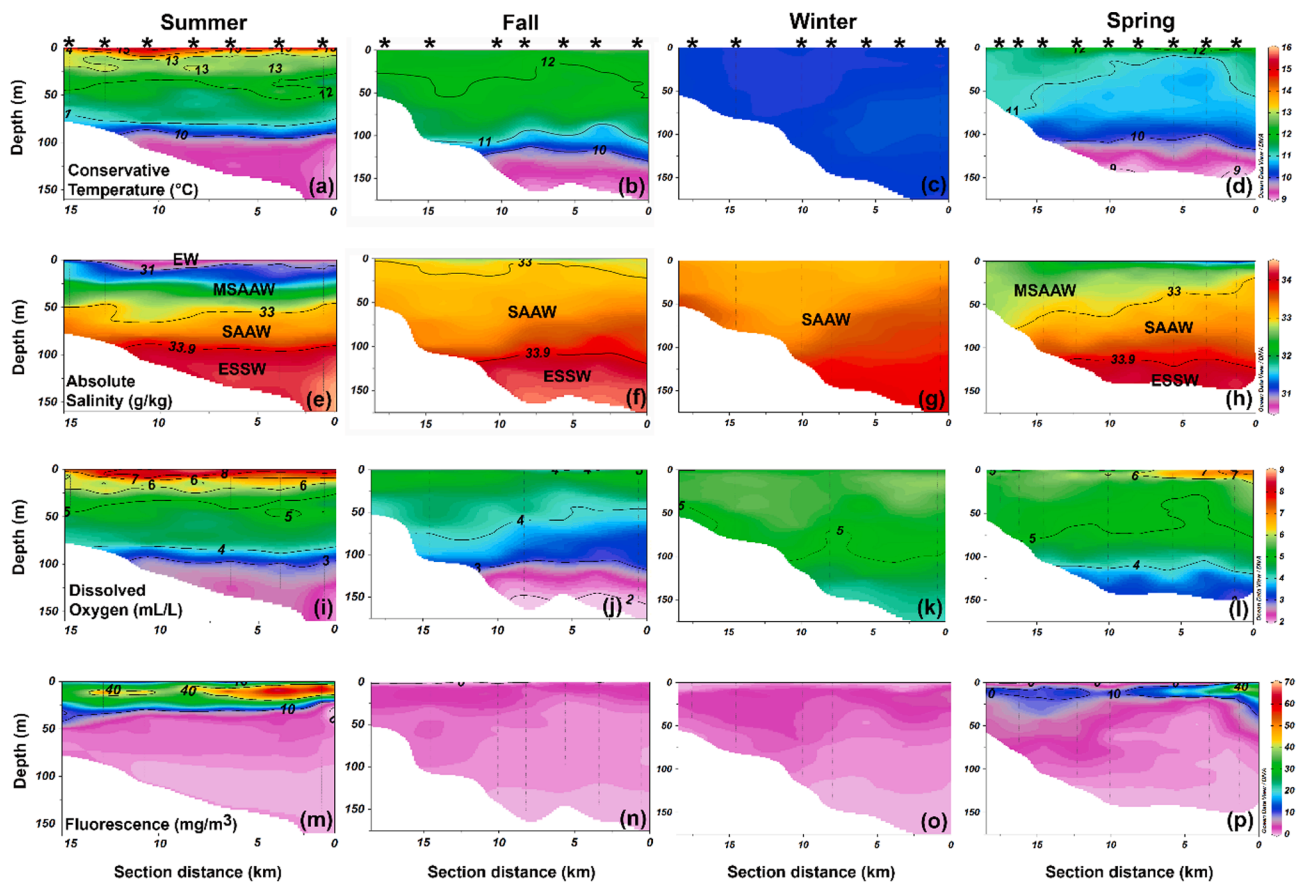


Fig. 8. Seasonal cross-sections (over-15 km) of the (a-d) conservative temperature ( $^{\circ}\text{C}$ ), (e-h) absolute salinity (g/kg), (i-l) dissolved oxygen (mL/L), and (m-p) chlorophyll fluorescence ( $\text{mg}/\text{m}^3$ ) for Summer (January), Autumn (April), Winter (June) and Spring (November) 2016. Note: 0 km marks the mooring site and stars above the panels indicate the location of each CTD profile. MSAAW: Modified Subantarctic Water; SAAW: Subantarctic Water; ESSW: Equatorial Subsurface Water.

concentrations and summertime blue whale occurrence. As the austral summer progressed, integrated water column zooplankton backscatter peaked (early February and late March 2016), approximately 1 month before the peak in blue whale song call rates (April). This peak in acoustic presence may either indicate a peak in animal aggregation (a higher number of animals) and/or an increase in individual call rates (more sound production per animal). There is currently limited information on the seasonal variation of sound production in blue whales, but recent studies of blue whales off California have shown increased sound production in tagged animals in autumn vs. summer (Lewis et al., 2018), seasonal changes in diel calling behavior in tagged animals (Oestreich et al., 2020), and different seasonal onsets and cessations of D-call and song calls (Szesciorka et al., 2020). There is some evidence, however,

that higher numbers of blue whales aggregate in the NCP at the end of summer based on visual sightings (Hucke-Gaete et al., 2004). In either case, high call rates may be linked to high euphausiid biomass a month prior because increased prey biomass may lead to the greater aggregation of blue whales and/or more energy available to individual whales for increased song production.

After April, blue whale call rates and zooplankton backscatter start dropping off, coinciding with decreased primary and secondary productivity reported by other authors (Iriarte et al., 2007; González et al., 2010, 2011; Buchan and Quiñones, 2016). Zooplankton backscatter was low from June 2016 onwards, when acoustic presence also dropped to very low levels. Hucke-Gaete et al. (2018) reported that the onset of migration of satellite-tagged blue whales out of NCP occurred from mid-

autumn to early winter. Hydrographic data showed that surface chlorophyll fluorescence is lower in April, the water column is more mixed and the influence of MSAAW much less; by June, fluorescence is low, the water column is well-mixed, and SAAW dominates. Nutrient profiles also reflect the lack of phytoplankton nutrient uptake in surface layers and a well-mixed water column in autumn and winter (Supplementary Materials Fig. 2).

A recent study by [Abrahms et al. \(2019\)](#) suggests that blue whales rely on their memory of long-term average productivity conditions to time their seasonal migrations. [Szesciorka et al. \(2020\)](#) also found evidence to support this hypothesis and show that arrival times over a ten year period of blue whales on their feeding ground is related to environmental variables from the previous feeding season. Our results therefore may be explained by blue whales in NCP timing their arrival on the feeding ground in response to memory of the seasonal increase in prey biomass (temporal lag observed between increased prey and onset of acoustic presence), and timing their departure when they detect the seasonal decrease of prey (no clear temporal lag observed).

#### 4.2. Intraseasonal and submonthly variation in blue whale acoustic presence and prey backscatter

Over the feeding season, the GLM response curve of predicted blue whale acoustic presence and backscatter (integrated, 50 m and 100 m), and the low Akaike information coefficients for these GLMs, indicate that blue whale submonthly presence was associated with euphausiid biomass in the water column. Both song calls and D-calls had a highly statistically significant relationships with backscatter, however this may be driven by a seasonal effect in the case of song calls and a submonthly effect in the case of D-calls. In contrast to song calls, D-calls did not display a strong seasonal signal (rise and fall between January and June), but rather two peaks that coincided with peaks in backscatter, particularly with backscatter at 50 m. Where GLMs provided insights into drivers of temporal distribution of blue whale acoustic presence over the entire 6-month summer feeding season (January to June), wavelet analyses allowed examination of smaller temporal scales (<1 month) that can be missed by pooling all the data together in GLMs. At the submonthly scale, wavelet transforms of D-calls revealed periodicities that coincided temporally (April and May) with periodicities of integrated backscatter, backscatter at 50 m, tidal amplitude, and meridional wind stress in the range of 14–18 days, and with zonal and meridional wind stress for periods in the 4–8 day range. Song calls and backscatter at 100 m had little or no significant submonthly periodicity.

These results suggest that whereas song calls follow a seasonal trend that lags behind and is linked to seasonal euphausiid population growth (discussed in the previous section), D-calls maybe a response to short term variations in euphausiid aggregation over submonthly cycles. Based on limited evidence in the literature, D-calls are thought to be indicative of blue whale in close proximity during a range of behaviors, including feeding (e.g., [Oleson et al., 2007a, 2007b](#); [Lewis et al., 2018](#)). Our results certainly suggest that D-calls are related to feeding; but feeding and socializing may not be mutually exclusive in blue whales. Animals may take advantage of close proximity with conspecifics at an euphausiid prey patch to socialize. Even reproductive behavior may not be mutually exclusive on feeding grounds at certain times of year, as recent work by [Schall et al. \(2020\)](#) shows possible reproductive behavior associated with the production of D-calls in late summer in NCP. More research is undoubtedly needed on the function of D-calls, but they could be used as a proxy for whale aggregation in the future. What is apparent is that D-calls may be more useful than song calls for understanding timing and processes related to prey/whale aggregations within a feeding season. In effect, [Szesciorka et al. \(2020\)](#) off California, suggest that the environmental drivers have a much greater influence on the production of D-calls vs. song calls.

Over the feeding season, the GLM response curve of blue whale acoustic presence and tidal amplitude suggests that tidal forcing

(transport and mixing) might contribute to prey aggregation and/or transport into the Corcovado Gulf, which in turn leads to increased blue whale presence. Tidal cycles have been found to cause changes in zooplankton abundance and community composition (e.g., [Cotté and Simard, 2005](#); [Gómez-Gutiérrez and Robinson, 2006](#); [De Melo et al., 2007](#); [Castro et al., 2011](#); [da Costa et al., 2013](#); [Etilé et al., 2015](#)). On a blue whale feeding ground in the St. Lawrence Estuary, [Cotté and Simard \(2005\)](#) found that euphausiids were transported further inside the estuary during flood tides and that this transport plus local upwelling led to dense aggregations. In addition to semi-diurnal effects, transport is increased during spring tides (e.g. [Gómez-Gutiérrez and Robinson, 2006](#); [De Melo et al., 2007](#)). [Gómez-Gutiérrez and Robinson \(2006\)](#) found that highest euphausiid transport into a shallow bay in Mexico occurred during the flood phase of spring tides, but transport was also dependent on euphausiid abundance over the continental shelf, indicating the importance of considering connections between the inner sea and shelf areas for future studies in NCP.

From the GLM analysis, there was no evidence of a relationship between whale acoustic presence and either meridional or zonal wind stress was found during the summer feeding season. In contrast to tidal amplitude which is a consistent physical forcing with marked periodicity throughout the time series, periodicity in wind stress “switches on and off” throughout the summer season, as reflected by the wavelet transforms. This may explain a lack of significant coefficients in the GLM analysis, however wind stress may still play an important role in driving blue whale acoustic presence during certain times of the feeding season. [Barlow et al. \(2021\)](#) analyzed the effect of wind on blue whale aggregation in New Zealand on an event-by-event basis. In effect, wavelet coherence revealed moderate (>0.6 magnitude-squared) and high correlations (>0.8 magnitude-squared) between D-calls and wind stress (zonal and meridional) over cycles of 14–24 days and 4–8 days during short time windows throughout the time series, particularly in April and May ([Fig. 7](#)). Wind stress variability occurred primarily over a 16.5-day cycle, but also a 27.5-day cycle, and shorter cycles of 2–8 days associated to low pressure systems (storms) and other atmospheric forcing such as the Baroclinic Annular Mode ([Ross et al., 2015](#); [Pérez-Santos et al., 2019](#); [Narváez et al., 2019](#)). The near 16-day and 27-day periods may also be compounded by similar tidal periods associated to the spring-neap tidal cycle. Wind stress variability indicates strong winds events in both meridional and zonal components, which leads to vertical mixing in the water column, which in turn is known to increase primary productivity in this area ([Montero et al., 2017](#); [Pérez-Santos et al., 2019](#)). Water column mixing during strong wind events provides nutrient input into the euphotic layer, which together with solar radiation and subsequent water column stability when winds relax, are the necessary conditions for phytoplankton growth. The development of phytoplankton blooms can in turn lead to euphausiid aggregation around these blooms and trigger blue whale feeding events.

#### 4.3. Coupling passive and active acoustic data

The spatial scales over which hydrophones and oceanographic instruments monitor the ocean environment must be considered when coupling PAM and oceanographic data. For this coastal study site, detection range was estimated at between 2.75 km and 15.3 km for song calls and 1.4 to 6 km for D-calls. Detection range for D-calls was smaller given the lower source levels and higher frequencies of D-calls ([Berchok et al., 2006](#); [Samaran et al., 2010a, 2010b](#)). These values are considerably less than those reported for the open ocean (e.g. [Samaran et al., 2010a, 2010b](#)). The mooring was in a small basin with a land mass nearby and subsurface bathymetric rises that constrained how far away a low-frequency whale call could be heard ([Fig. 1a](#)). This detection range is still greater than the spatial scales of monitoring for backscatter, which are measurements taken at a single point of observation. This means that we must interpret these results with caution because whales calling 15 km away from the mooring may not necessarily be feeding on

prey patches at the mooring. However, Santora et al. (2009) found that euphausiid patch extension in the Southern Ocean was between 1 and 9 nautical miles, and Benoit-Bird et al. (2013) found that euphausiid patches in the Bering Sea varied over 5–10 km. Net sampling in our study area at sampling stations 10–30 km apart during the austral winter and spring showed similar levels of high euphausiid densities across four consecutive sampling stations (Cisternas, 2011). These studies suggest that backscatter measurements at a single point may be representative of a patch that is at least a few km in size and possibly well over 10 km. Future characterization of the spatial variation of prey patches in this area will be necessary to fully inform the coupling of backscatter and blue whale acoustic presence data.

With these limitations in mind, our results still suggest that during certain time windows of the summer feeding season, events of increased wind stress with periodicities from days to 1 month, may contribute to the aggregation of prey and blue whales on their feeding ground. Wind stress and tidal cycles may also interact and amplify this effect. More work is needed to gain a mechanistic understanding of the effects of tidal cycles, wind stress and other physical drivers on prey aggregation in NCP.

## 5. Conclusions

Understanding the functioning of highly dynamic estuarine systems, and how large predators like blue whales respond to temporal changes in these feeding habitats, is challenging. *In situ* oceanographic time series coupled with continuous PAM data is a more traditional oceanographic research approach than is not often used to study marine mammals. This approach can reveal dynamic and complex patterns to help gain insights into the drivers of whale occurrence over a range of temporal scales.

The results of this study indicate that the seasonal presence of blue whales on their feeding ground is a response to seasonal variation in euphausiid prey biomass. Over the summer feeding season, blue whale acoustic presence was strongly associated with zooplankton backscatter (GLM coefficient  $p < 0.0001$ ). There is a lag of several months between the onset of high euphausiid biomass and the arrival blue whales, and an almost immediate departure of blue whales once biomass decreases. Results also suggest that song calls and D-calls, the two types of vocalization produced by blue whales, may respond to environmental drivers over different timescales. Song calls, which are thought to be long-range communications that serve as some sort of reproductive display, appear to follow a seasonal cycle, i.e. rise and fall over the summer feeding season (January and June). D-calls on the other hand, which are thought to be produced when blue whales are in close proximity, appear to respond quickly to short term variations in the environment that may aggregate prey over submonthly cycles. This suggest that D-calls are produced during feeding and/or when animals that have aggregated whilst feeding engage in social interactions. There was also an association between blue whale acoustic presence and tidal amplitude ( $p < 0.05$ ), suggesting that spring tides might increase prey aggregation and/or transport into the Corcovado Gulf, leading to increased blue whale acoustic presence over 15-day or 30-day cycles. Wavelet and wavelet coherence analyses suggest that during certain time windows of the summer feeding season, short-lived events of increased wind stress with periodicities from days to 1 month, may contribute to the aggregation of prey, causing increased D-call presence.

This study provides novel information on the drivers of seasonal and submonthly Southeast Pacific blue whale (acoustic) presence on the mega-estuarine feeding ground in NCP, relevant for developing conservation measures to ensure protection for Endangered Chilean blue whales. This study also shows how passive and active acoustic approaches can be coupled, with certain inherent limitations, to examine the functioning of pelagic ecosystems used by large whales as feeding grounds. We hope that this work encourages the use of PAM in oceanographic studies to determine long-term patterns in the response of

pelagic predators to changing ocean productivity. This is increasingly important in NCP and globally under projected global climate change scenarios.

## Declaration of Competing Interest

The authors declare that they have no known competing financial interests or personal relationships that could have appeared to influence the work reported in this paper.

## Acknowledgements

Financial support was provided by Centro COPAS Sur-Austral ANID AFB170006 and COPAS Coastal FB10021 <https://www.anid.cl/>, and Office of Naval Research Global and Office of Naval Research grant N00014-17-1-2606. We thank the Centro de Investigación en Ecosistemas de la Patagonia (CIEP) for providing the meteorological sensors installed at the port of Melinka. We also thank the FIPA 2015-07 project awarded to IPS and the Ecoclimatico project CIEP R17A10002 awarded to CIEP for supporting fieldwork. Our sincere thanks to Gabriela Igor and Eduardo Escalona for their valuable help in the field with sample collection. Thanks to Camila Calderon for help with preparation of Fig. 5. We are very grateful to the captains and crews of Maranata and Don Felipe for their valuable support during fieldwork. Our sincere thanks to the anonymous reviewers whose comments greatly improved the quality of our work, and particularly Dr. David Cade for his careful review and valuable advice regarding the backscatter analysis.

## Author contributions

SJB contributed to study conception, design, data collection and analysis, manuscript preparation, including writing the first draft of this manuscript, and securing funding. IPS contributed to study conception, design, data collection and analysis, manuscript preparation, and securing funding. DN and AVL contributed to study design, data analysis and manuscript preparation. MB and KS contributed to data analysis, manuscript preparation, and securing funding. LC contributed to study design, data collections and analysis, and manuscript preparation. LG and CR contributed to data analysis. PM contributed to data collection and analysis, and manuscript preparation. JP contributed to data analysis and manuscript preparation. GD contributed to manuscript preparation. SN contributed to securing funding and manuscript preparation. All authors commented on all previous versions of the manuscript and read and approved the final manuscript.

## Contribution to the field

This study provides a better understanding of the pelagic ecology of a blue whale feeding ground in mega-estuarine systems and reinforces the importance of this seasonal feeding ground for Endangered Southeast Pacific blue whales.

This study demonstrates how Passive Acoustic Monitoring (PAM) of whales and hydroacoustic monitoring of zooplankton can be integrated to understand the ecological dynamics of feeding grounds, as well as provide a basis for the monitoring of whale acoustic presence to be used in the future as a means of monitoring long-term patterns in ocean productivity. This is increasingly important in NCP and globally under projected global climate change scenarios.

## Appendix A. Supplementary material

Supplementary data to this article can be found online at <https://doi.org/10.1016/j.pcean.2021.102709>.



